Chemistry–A European Journal
Research Article
doi.org/10.1002/chem.202103883
Chemistry Europe
European Chemical Societies Publishing
www.chemeurj.org

# Structural and Functional Analysis of Bacterial Sulfonosphingolipids and Rosette-Inducing Factor 2 (RIF-2) by Mass Spectrometry-Guided Isolation and Total Synthesis

Daniel Leichnitz[+],[a] Chia-Chi Peng[+],[a] Luka Raguž,[a] Florentine U. N. Rutaganira,[b] Theresa Jautzus,[a] Lars Regestein,[c] Nicole King,[b] and Christine Beemelmanns*[a]

**Abstract:** We have analyzed the abundance of bacterial sulfonosphingolipids, including rosette-inducing factors (RIFs), in seven bacterial prey strains by using high-resolution tandem mass spectrometry (HRMS$^2$) and molecular networking (MN) within the Global Natural Product Social Molecular Networking (GNPS) web platform. Six sulfonosphingolipids resembling RIFs were isolated and their structures were elucidated based on comparative MS and NMR studies. Here, we also report the first total synthesis of two RIF-2 diastereomers and one congener in 15 and eight synthetic steps, respectively. For the total synthesis of RIF-2 congeners, we employed a decarboxylative cross-coupling reaction to synthesize the necessary branched α-hydroxy fatty acids, and the Garner-aldehyde approach to generate the capnine base carrying three stereogenic centers. Bioactivity studies in the choanoflagellate *Salpingoeca rosetta* revealed that the rosette inducing activity of RIFs is inhibited dose dependently by the co-occurring sulfonosphingolipid sulfobacins D and F and that activity of RIFs is specific for isolates obtained from *Algoriphagus*.

## Introduction

Choanoflagellates, the closest known living single-celled relatives of animals, are water-dwelling predators of bacteria that have emerged as new model systems for studying eukaryotic development.[1,2] While predominately unicellular, several choanoflagellate species such as *Salpingoeca rosetta* have multicellular-like life stages, including rosettes, that are formed upon sensing of specific signaling biomolecules released by their prey bacteria (Figure 1).[3–5] The bacterial signals responsible for the morphological switch in *S. rosetta* were identified as specific sulfonosphingolipids (rosette-inducing factors, RIFs) produced by the co-occurring prey bacterium *Algoriphagus machipongonensis*.[6,7] Isolated RIF-1 and RIF-2 induced rosette formation in a small subfraction of all cells, and a mixture of inducing RIFs, including yet unidentified congeners, promoted

[a] *D. Leichnitz,[+] C.-C. Peng,[+] L. Raguž, T. Jautzus, Dr. C. Beemelmanns*
*Chemical Biology of Microbe-Host Interactions*
*Leibniz Institute for Natural Product Research*
*and Infection Biology – Hans-Knöll-Institute (HKI)*
*Beutenbergstraße 11a, 07745,*
*Jena (Germany)*
*E-mail: Christine.Beemelmanns@hki-jena.de*

[b] *Dr. F. U. N. Rutaganira, Prof. N. King*
*Life Sciences Addition,*
*University of California, Berkeley*
*Berkeley, CA*
*94720 (USA)*

[c] *Dr. L. Regestein*
*Bio Pilot Plant*
*Leibniz Institute for Natural Product Research*
*and Infection Biology – Hans-Knöll-Institute (HKI)*
*Beutenbergstraße 11a, 07745,*
*Jena (Germany)*

[+] *These authors contributed equally to this work.*

*Supporting information for this article is available on the WWW under https://doi.org/10.1002/chem.202103883*



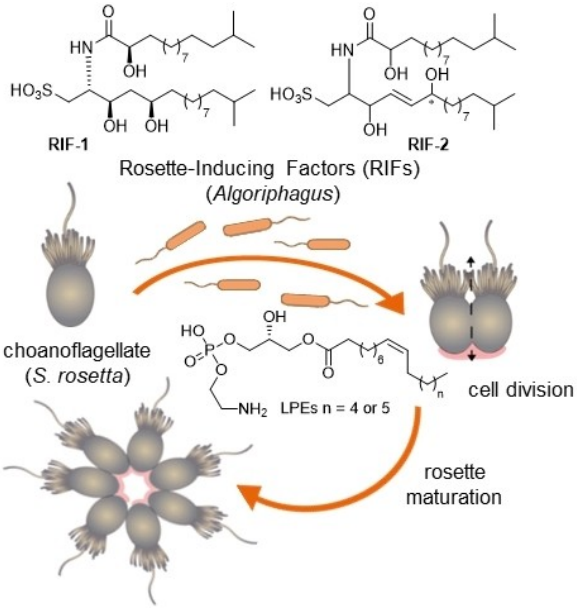


**Figure 1.** Cross-kingdom interactions between *S. rosetta* and *A. machipongonensis*. Bacterial sulfonosphingolipids trigger the morphological switch from single cells to rosette-like colonial cell type.

rosette development in 20–30% of cells.[7] *A. machipongonensis* also produced two lysophosphatidylethanolamines (LPEs), metabolic intermediates in bacterial phospholipid turnover and known signaling molecules,[8] which synergized with RIFs to enhance rosette development in about 80% of all cells.[7,9] These chemically/ecologically driven studies exemplified that a specific set of bacterial membrane lipids, which are structurally highly related to eukaryotic signaling molecules,[10–14] can act as cross-kingdom signals and induce developmental changes in the eukaryotic recipient.[15]

The tight structure-activity relationship of RIFs raised intriguing questions about the abundance and morphogenic activities of RIF-like metabolites derived from other known prey bacteria.

Here, we questioned to what extent RIFs, related sulfonosphingolipids, and LPEs are produced by Bacteroidetes species (*Algoriphagus* spp., *Cyclobacterium marinum*, *pacifica*) previously evaluated within the interaction with *S. rosetta* (Tables S4 and S5 in the Supporting Information).[4] Thus, we set out to pursue a high-resolution tandem mass spectrometry (HRMS$^2$)- and Global Natural Product Social Molecular Networking (GNPS)-based[16] metabolomic analysis of bacterial prey species and aimed to complement the analysis by a total synthesis of RIF-2 to verify its structural assignment and if possible, deduce RIF-2's absolute stereochemistry.[7]

## Results and Discussion

### Sulfonolipid isolation

First, we pursued a comparative HRMS$^2$-based GNPS analysis of five rosette-inducing *Algoriphagus* species (*A. machipongonensis* PR1, *A. aquimarinus* LMG 21971, *A. ratkowskyi* LMG 21435, *A. marincola* SW-2, *A. antarcticus* LMG 21980, Table S1), which revealed overall highly similar sulfonolipid and LPE profiles across all species (Figures 2 and S1–S10).[6,7] Whereas signals for RIF-1 (*m/z* 606.441 [*M*−H]$^-$) and RIF-2 (*m/z* 604.425 [*M*−H]$^-$) were found only in very low abundance, non-inducing sulfonosphingolipids like sulfobacin B, D and F (*m/z* 574.451,

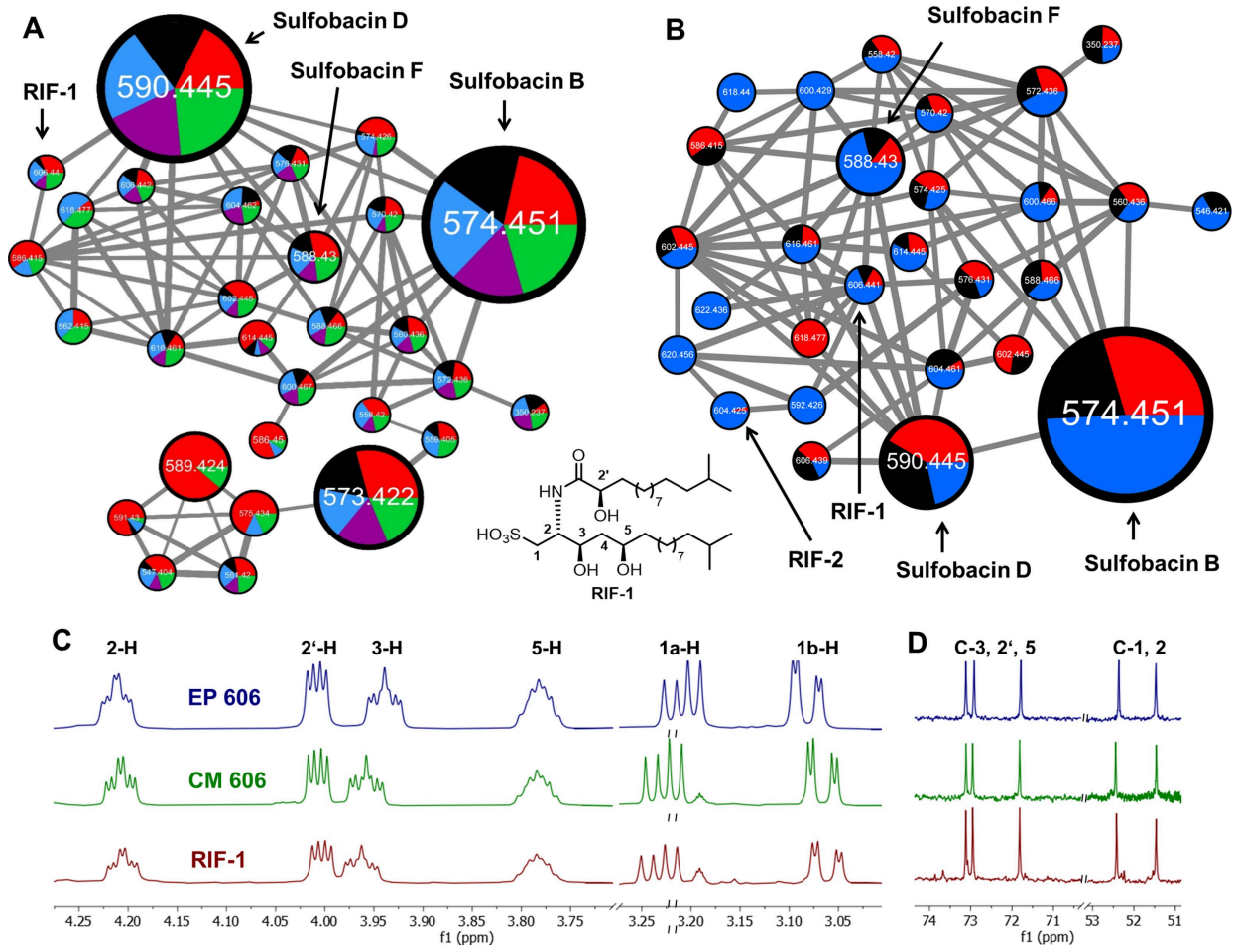


**Figure 2.** HRMS$^2$-based GNPS cluster (negative ion mode) of cell membrane extracts with nodes for RIF-1 (*m/z* 606.441 [*M*−H]$^-$), RIF-2 (*m/z* 604.425 [*M*−H]$^-$), sulfobacin F (*m/z* 588.430 [*M*−H]$^-$), sulfobacin D (*m/z* 590.445 [*M*−H]$^-$), sulfobacin B (*m/z* 574.451 [*M*−H]$^-$) in A) *A. machipongonensis* PR1 (red), *A. antarcticus* LMG 21980 (black), *A. marincola* SW-2 (blue), *A. ratkowskyi* LMG 21435 (purple) and *A. aquimarinus* LMG 21971 (green) and B) *A. machipongonensis* PR1 (red), *C. marinum* LMG 13164 (black) and *E. pacifica* KMM 6172 (blue). Stacked C) $^1$H and D) $^{13}$C NMR spectra ($CD_3OD$, 600 MHz) of EP-606 (blue), CM-606 (green), and RIF-1.

590.445, and 588.430 [$M-H]^-$) dominated the sulfonolipid profiles.[6] An LPE-related GNPS cluster was detected in all five strains with synergizing LPE-450 (*m/z* 450.263 [$M-H]^-$) and LPE-464 (*m/z* 464.278 [$M-H]^-$) being produced by most of the tested bacterial strains.

We then compared the sulfonosphingolipid profile of rosette-inducing *C. marinum* LMG 13164 with *A. machipongonensis* PR1 and the non-inducing prey species *E. pacifica* KMM 6172. As shown in Figure 2B, rosette-inducing bacteria *A. machipongonensis* and *C. marinum* share a highly similar sulfonolipid-related molecular ion pattern with the non-inducing strain *E. pacifica* including *m/z* signals assigned to RIF-1 and RIF-2. An LPE-related GNPS cluster with nodes corresponding to LPE-450 (*m/z* 450.263 [$M-H]^-$) and LPE-464 (*m/z* 464.278 [$M-H]^-$) was observed in all three strains.

To clarify if the detected molecular ions assigned to sulfobacin F (*m/z* 588.430 [$M-H]^-$), RIF-1 (*m/z* 606.441 [$M-H]^-$) and RIF-2 (*m/z* 604.425 [$M-H]^-$) in *C. marinum* and *E. pacifica* relate to the same stereoisomers as those characterized from *A. machipongonensis*,[6,7] we pursued an MS-guided purification of lipid extracts (Figure S11, Table S2).

Sulfonosphingolipids, which were isolated from *E. pacifica* and *C. marinum* and showed the same molecular mass as RIF-2 (*m/z* 604.425 [$M-H]^-$) were assigned as CM-604 and EP-604, respectively. Similarly, sulfonosphingolipids having the same molecular mass as RIF-1 (*m/z* 606.441 [$M-H]^-$) were assigned as CM-606 and EP-606, while sulfobacin F congeners with an *m/z* 588.430 [$M-H]^-$ were named CM-588 and EP-588, respectively.

We then compared the 1D NMR data obtained from RIF-2, EP-604 and CM-604 (Tables S3 and S4, $CD_3OD$ or [$D_6$]DMSO) and observed nearly identical $^1H$ and $^{13}C$ chemical shift patterns as well as 2D correlations for all three compounds (Scheme 5, below), which suggested the same structural, and possibly, the same stereochemical assignment for all three isolated compounds.

Similarly, NMR-based comparison of isolated and synthetic RIF-1,[6] CM-606 and EP-606 (Figure 2C, Tables S8 and S9) unraveled almost identical chemical shifts and coupling constants, which again suggested the same relative stereochemistry of all three isolated compounds. A similar conclusion was inferred when NMR spectra of sulfobacin F like compounds (sulfobacin F, CM-588 and EP-588) were compared (Tables S10 and S11). The comparative NMR analysis was complemented by experimental CD measurements, which showed identical absorption patterns for each sulfonolipid-type (Figures S12–S14).

Thus, we hypothesized at this stage that sulfonosphingolipids from *C. marinum* and *E. pacifica* might be of the same stereochemical configuration as those derived from *A. machipongonensis*.

## Bioactivities

In a next step, we investigated the influence of the most abundant bacterial sulfonosphingolipids (sulfobacins D and F) on the rosette-inducing capacity of RIFs obtained from *A. machipongonensis* using *S. rosetta* cell lines that are kept in co-culture with a non-inducing bacterial prey *E. pacifica*.

As expected from previous studies, the addition of purified sulfonosphingolipids RIF-1 and RIF-2, as well as outer-membrane vesicles (OMVs) isolated from *A. machipongonensis* (positive control) reliably induced the formation of stable rosettes in a dose-dependent fashion without any sign of growth inhibition, while supplementation of either sulfobacin D or sulfobacin F caused no phenotypic change in *S. rosetta* (Figure 3A).[6]

However, addition of sulfobacin-like lipids to a constant concentration of inducing RIF-1 (10 μM) or RIF-2 (3 μM) resulted in a dose-dependent reduction in rosette formation (Figure 3B). A similar effect was also previously observed for the sulfonolipid-based inhibitor IOR-1A from *A. machipongonensis*.[5,7] Thus, structurally related sulfobacins D and F appear to act as competitive inhibitors of RIFs, and thus might also serve as a counter measure to avoid predation of *A. machipongonensis* by rosettes of *S. rosetta*.[6,7,17]

Next, we evaluated the inducing effects of RIF-like sulfonosphingolipids isolated from the non-inducer strain *E. pacifica* (EP-604 and EP-606) and the rosette-inducing strain *C. marinum* (CM-604 nor CM-606). To our surprise, none of the isolated RIF-like sulfonosphingolipids caused rosette formation at any given concentration, but instead, three RIF-like sulfonosphingolipids EP-604, CM-604 and CM-606 caused the reduction of cell density, despite their structural resemblance to RIF-1 and RIF-2 (Figure 3C).

## Total synthesis

To solve the contradicting structure-activity results (Figure 3D), we pursued the total synthesis of two RIF-2 diastereomers having either *S* or *R* configuration at C-6. The remaining stereocenters at C-2, C-3 and C-2′ were anticipated to be determined as (2*R*,2′*R*,3*R*) due to the conserved sphingolipid biosynthesis and were also previously verified in sulfonosphingolipid syntheses of RIF-1 and sulfobacins.[18,19] Inspired by our previous synthetic studies and earlier reports on structurally related 6-hydroxy sphingosine or 6-hydroxy ceramides[20–24] we envisaged building up the capnine base by the alkynylation of Garner's aldehyde using prochiral propargylic ketones and/or enantiopure propargylic alcohols (Scheme 1). Although the

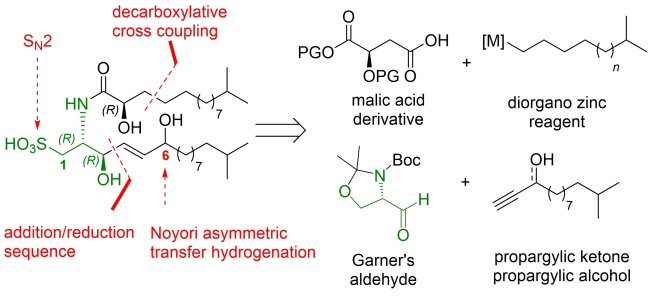


**Scheme 1.** Retrosynthetic considerations for RIF-2.

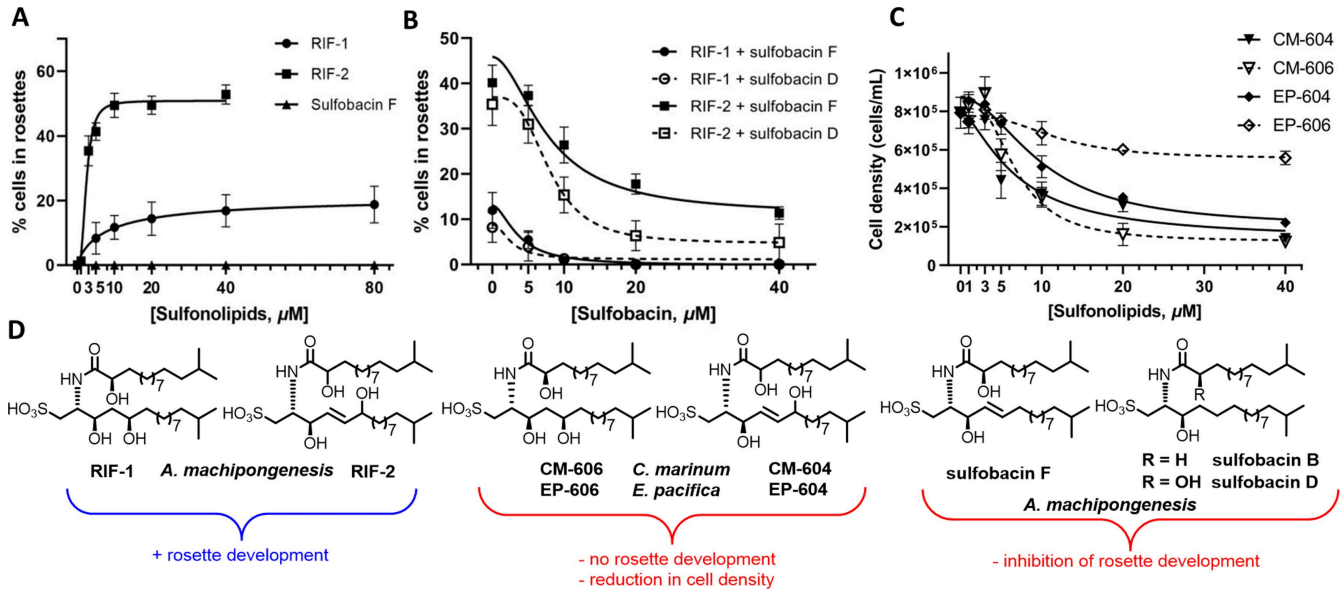


**Figure 3.** A) Rosette development of *S. rosetta* in the presence of increasing concentrations of RIF-1, RIF-2 and sulfobacin F. B) Rosette development of *S. rosetta* in the presence of RIF-1 (10 μM) or RIF-2 (3 μM) and increasing concentration of sulfobacin D and F, respectively. C) Cell density of *S. rosetta* in the presence of increasing concentrations of EP-604, EP-606 and CM-604 and CM-606. Outer-membrane vesicles (OMVs) from A. *machipongonensis* PR1 served as positive and DMSO as negative control (data not shown). D) Structures of sulfonosphingolipids isolated from *A. machipongonensis* PR1, *C. marinum* LMG 13164 (CM) and *E. pacifica* KMM 6172 (EP).

outlined strategy would require a stereoselective reduction of the triple bond at the final stage of the synthesis, it allows for the use of acidic and oxidative reaction conditions to introduce the sulfono-headgroup.

In a first step, we analyzed options for a step-effective synthesis of the α-hydroxy-fatty acid as many enantioselective approaches required the use of auxiliaries, protecting group sequences and final oxidation steps to the acid.[6,25] To explore new synthetic avenues, we decided to make use of a recently described Ni-catalyzed decarboxylative cross-coupling strategy,[26,27] and treated acetonide-protected malic acid **1** (single step from D-malic acid) with di(10-methylundecyl)zinc as coupling partner, which afforded fatty acid **3** in not yet optimized 19% yield after deprotection (Scheme 2).[28,29] Functionalized acid **4** was obtained in a similar fashion in 18% yield in only two synthetic steps. Despite the low yields, the remarkably short reaction sequence motivated us to explore a reaction sequence that would allow for the formation of a silyl-protected fatty acid. Hence, TIPS-protected methyl ester **5** (2 steps from malic acid, 48% yield) was reacted with dipentadecylzinc under decarboxylative cross-coupling conditions which afforded the desired product in 54% yield. Subsequent saponification yielded the linear fatty acid **6** in 12% yield over two steps. To avoid by-product formation and allow for modifications upon demand, di(oct-7-en-1-yl)zinc was used as a coupling partner for the cross-coupling reaction affording methyl ester **7** in 32% yield. The desired elongated and branched fatty acid **8** was obtained by cross metathesis, reduction of the double bond and saponification in 95% yield over three steps. Overall, despite moderate yields for decarboxylative cross-coupling reactions, the reaction sequences allow

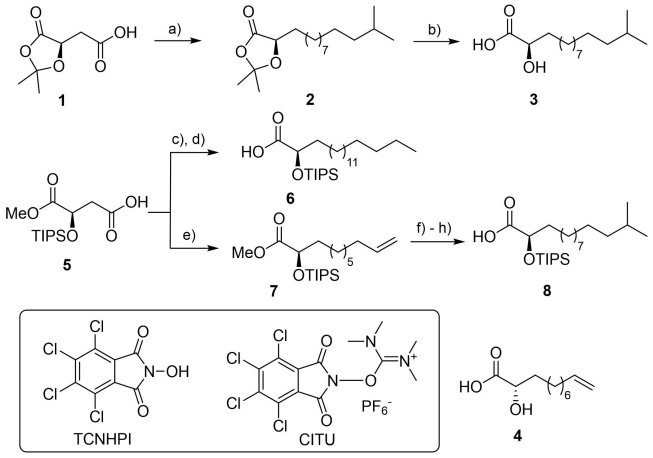


**Scheme 2.** Synthesis of α-hydroxylated fatty acids. a) CITU, NMM, DMF, RT, 10 min, then $NiCl_2$·glyme, 4,4′-di-*t*Bu-bpy, DMF, di(10-methylundecyl)zinc, THF, RT, 16 h, 32%; b) 1 M HCl, THF/$H_2O$, 110 °C, 5 min; 59%; c) DIC, TCNHPI, 4-DMAP, $CH_2Cl_2$, RT, 10 min, then $NiCl_2$·glyme, 4,4′di-*t*Bu-bpy, DMF, dipentadecylzinc, THF, RT, 16 h, 54%; d) LiOH, THF/MeOH/$H_2O$, 0 °C to RT, 16 h, 23%; e) CITU, NMM, 10 min, then $NiCl_2$·diglyme, 4,4′-di-*t*Bu-bpy, DMF, di(oct-7-en-1-yl)zinc, THF, RT, 16 h, 32%; f) Hoveyda-Grubbs catalyst 2nd-generation, 4-methylpent-1-ene, $CH_2Cl_2$, 40 °C, 3 h, 98%; g) $H_2$, Pd/C, EtOAc, RT, 1 h, 97%; h) LiOH, THF/MeOH/$H_2O$, 0 °C to RT, 16 h, quant.

for the direct synthesis of the free acid from the chiral pool without use of an auxiliary and/or oxidation to the acid.

The synthesis of the capnine base commenced with the diastereoselective addition (Felkin-Anh model) of the protected propargylic ketone **9** to Garner's aldehyde (Scheme 3).[30] Subsequent protection of the secondary alcohol and deprotection of the ketone afforded **11** over three steps in more than

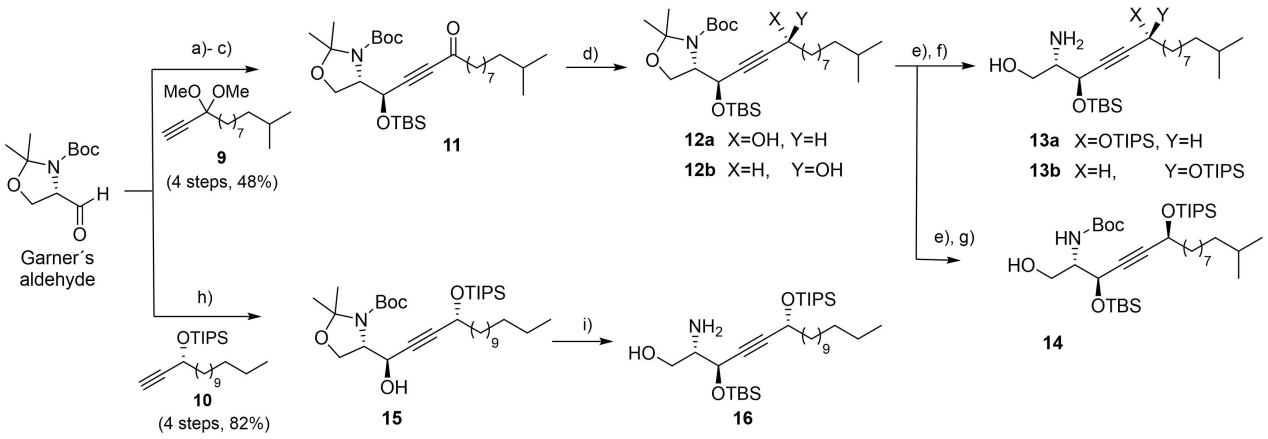


**Scheme 3.** Synthesis of capnine bases. a) *n*BuLi, **9**, THF/DMPU, −78 °C to RT, 16 h, 65%; b) TBSCl, DIPEA, DMF, RT, 16 h, 87%; c) *p*-toluene sulfonic acid (10 mol%), acetone, RT, 3 h, 98%; d) for **12a**: RuCl[(*R*,*R*)-TsDPEN](mesitylene) (5 mol%), FA, $Et_3N$, *i*PrOH, RT, 7 h, 37%; for **12b**: RuCl[(*S*,*S*)-TsDPEN](mesitylene) (5 mol%), FA, $Et_3N$, *i*PrOH, RT, 30 min, 63%; e) for **13a**: 1) TIPSOTf, 2,6-lutidine, $CH_2Cl_2$, 0 °C to RT, 16 h, 88%; 2) TMSOTf, 2,6-lutidine, $CH_2Cl_2$, 0 °C, 5 h, 69%; for **13b**: 1) TIPSOTf, 2,6-lutidine, $CH_2Cl_2$, 0 °C to RT, 16 h, 80%; 2) TMSOTf, 2,6-lutidine, $CH_2Cl_2$, 0 °C, 4 h, 50%; g) PPTS, MeOH, 60 °C, 1 h, 22% (66% brsm); h) *n*BuLi, **10**, THF/DMPU, −78 °C to RT, 16 h, 47%, *dr* > 19:1; i) TBSOTf, 2,6-lutidine, $CH_2Cl_2$, 0 °C, 5 h, then TMSOTf, 0 °C to RT, 3 h, 27%.

55% yield. We then applied Noyori's asymmetric hydrogen transfer protocol to reduce the ketone group.[31] While a matched effect was observed for the *S*,*S* enantiomer of the ligand yielding alcohol **12b** within 30 min at room temperature in 63% yield, a mismatched effect was observed for the *R*,*R* enantiomer resulting in **12a** in only 37% yield after 7 h. Here, it needs to be noted that we did not pursue a selective reduction of the triple bond at this stage as the resulting double bond derivative proved unstable towards later used deprotection-oxidation sequences. Thus, as next steps, the secondary alcohol was TIPS-protected using TIPSOTf and 2,6-lutidine, and the Boc group removed using our previously reported silyl triflate-induced cleavage to yield the free capnine bases **13a** and **13b**, respectively.[18] In addition, selective acetonide cleavage resulted in the formation of Boc-protected capnine base **14**.

Our second strategy employed the diastereoselective addition of the (3*R*)-propargylic alcohol **10** to Garner's aldehyde, which afforded **15** in moderate yields (47%, *dr* > 19:1). Boc-deprotection to the TBS-protected capnine base **16** was achieved in a similar fashion as shown for the branched compounds. At this stage of the synthesis, we considered ways to introduce the sulfonic acid at C-1. While nucleophilic replacement reactions of the primary alcohol with, for example, sodium sulfite were not successful,[17] conversion of model substrate **17** (*syn*-capnine base)[18] with thioacetate under Mitsunobu conditions resulted in the formation of thiol **19** (36% yield; Scheme 4). From a mechanistic point of view, the formation of an intermediate thioester **18** and subsequent acyl migration to form the stable amide bond appeared most likely. Motivated by the finding that thiol **19** was readily oxidized with $(NH_4)_6Mo_7O_{24}$ to sulfonic acid[20,32] we investigated shortly if longer acyl chains would undergo acyl-migration (thioligation). The required TIPS-protected thioacid **21** was obtained by treating fatty acid **8** with Lawesson's reagent in almost quantitative yield. In contrast, unprotected α-hydroxy acid formed stable but unreactive adducts with Lawesson's reagent (for details, see the Supporting Information SI-C12).

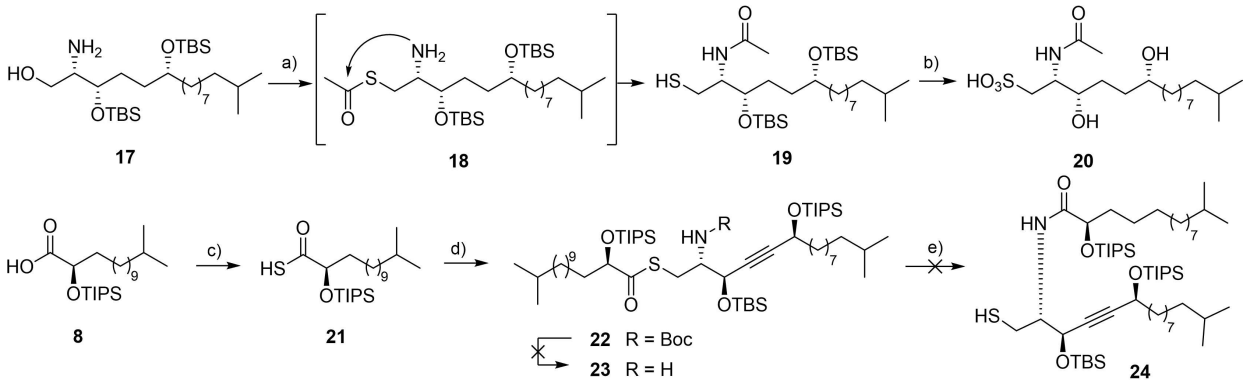


**Scheme 4.** Synthesis of thioester for native ligation-type reaction. a) $PPh_3$, DIAD, AcSH, $CH_2Cl_2$, 0 °C to RT, 16 h, 36%; b) $(NH_4)_6Mo_7O_{24}$, $H_2O_2$, MeOH, RT, 20 min, 11%; c) Lawesson's reagent, quant; d) **14**, $PPh_3$, DIAD, THF/$CH_2Cl_2$, 0 °C to RT, 27%; e) for tested conditions, see the Supporting Information.

To avoid spontaneous N-acylation, coupling of thioacid **21** was pursued with Boc-protected capnine base under Mitsunobu conditions yielding thioester **22** in moderate yields. To initiate the acyl-transfer, thioester **22** was first subjected to Boc-deprotection using TMSOTf;[33] however, neither deprotection nor migration of the acyl side chain was observed. Similar results were obtained with model substrates and reaction conditions known to selectively induce Boc-deprotection in the presence of silyl-protecting groups; in all cases either decomposition was observed or starting material recovered (Tables S1–S3).

In light of the low-yielding Mitsunobu coupling reaction with long-chain thioacids, we decided to reverse the reaction sequence by first acylating the capnine base and then pursuing the necessary substitution reaction at C-1 (Scheme 5A). Boc-deprotected capnine base **13a** was coupled with fatty acid **8** using peptide coupling conditions (HBTU in DMF) to yield **25a**, followed by the introduction of a thioacetate at C-1 under Mitsunobu conditions in good overall yield.[6] To allow for mild oxidation conditions, acetate protected thiol was deprotected with NaSMe[34] and then oxidized with *m*-CPBA in a one-pot fashion at 0 °C, which caused the simultaneous TBS-deprotection of the secondary alcohol yielding **26a**.[35] Although TBS-cleavage was preferred under the given reaction conditions, additional TIPS-deprotection (2′-position) was observed occasionally with prolonged reaction times. With propargyl alcohols

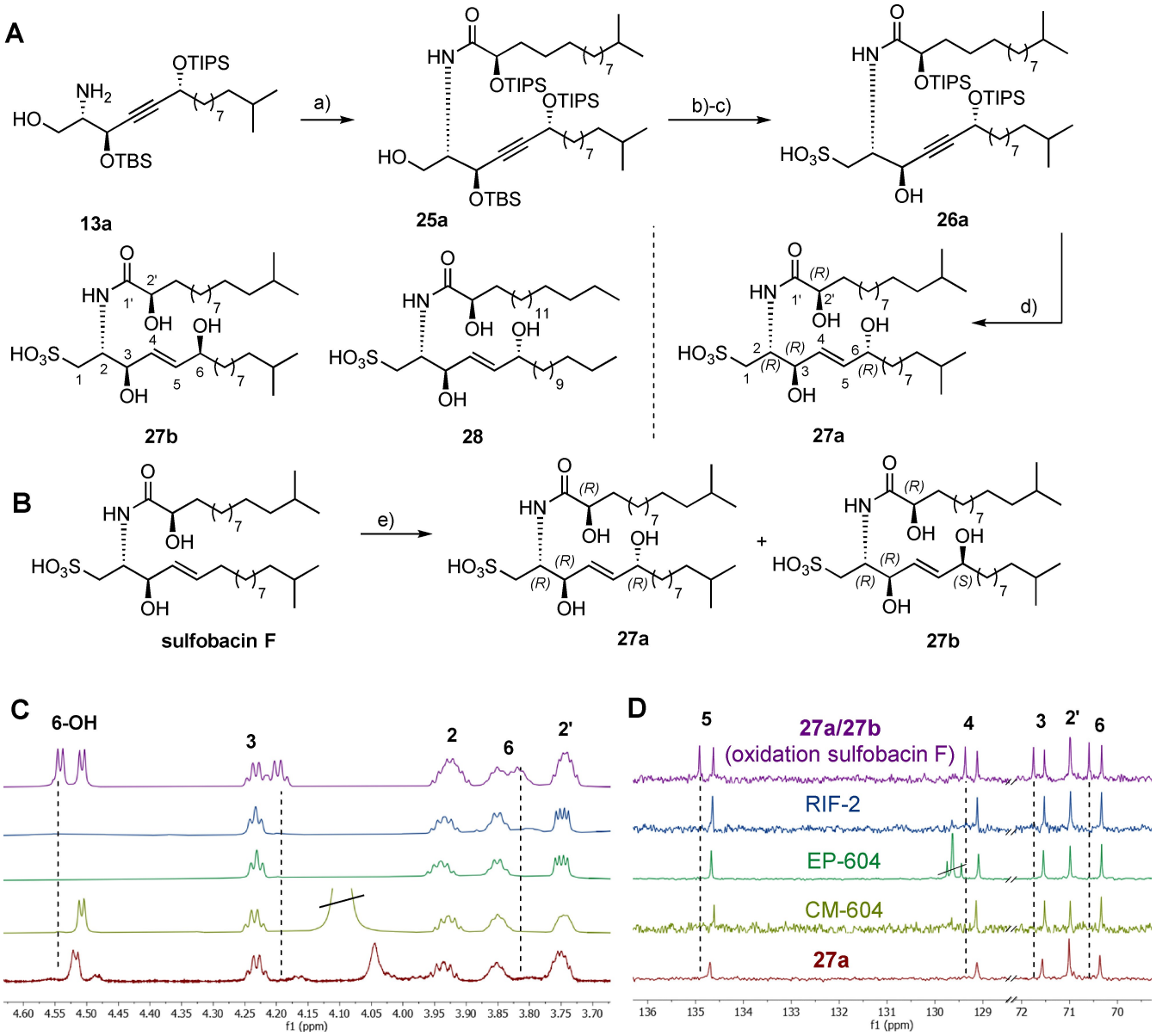


**Scheme 5.** A) Final steps in the synthesis of RIF-2 congeners: a) **8**, HBTU, DIPEA, DMF, 0 °C to RT, 1 h, 71%; b) $PPh_3$, DIAD, AcSH, THF/$CH_2Cl_2$, 0 °C to RT, 2 h, 73%; c) NaSMe, MeOH, 0 °C, 5 min, then *m*-CPBA, $CH_2Cl_2$, 0 °C, 5 min, then $SMe_2$, 0 °C, 5 min, 43%; d) Red-Al, THF, 0 °C, 6 h, 5.9%; B) Oxidation of sulfobacin F yielding **27a/27b**: e) $SeO_2$, 1,4-dioxane, $H_2O$, 130 °C, microwave, 4 h, 14%, *dr* (6*R*)-**27a**/(6*S*)-**27b** 1.7:1. Stacked C) $^1H$ and D) $^{13}C$ spectra ([$D_6$]DMSO, 600 MHz) of sulfonosphingolipids.

of type **26** in hands, the selective reduction of the triple bond was performed with Red-Al® and the remaining TIPS-groups were then removed with TBAF in THF. Here, it is important to note that the reduction step afforded in general higher yields if the hydroxy group at position 2′ and 6′ were TIPS protected. Overall, three sulfonosphingolipids were synthesized using the outlined synthetic route, including the 6*R* stereoisomer **27 a**, the 6*S* stereoisomer **27 b** (each required a total of 15 steps) and the unbranched 6*R* congener **28** (a total of eight steps). Comparison of NMR spectra of stereoisomer **27 a** (and **28**) showed a nearly perfect match to those of RIF-2 indicating a 6*R* stereochemistry (Tables S8 and S9).[36]

Based on the hypothesis that RIF-2 might originate from the selective enzymatic oxidation of the allylic position of the structural congener sulfobacin F, we also pursued a biomimetic approach and subjected sulfobacin F to Riley oxidation conditions (Scheme 5B),[22] which indeed yielded an inseparable mixture of sulfonic acids **27 a/27 b** in 14% yield.

To deduce the most likely stereochemical assignment of RIF-2, we compared $^{1}H$ and $^{13}C$ NMR spectra of synthesized and isolated RIF-2 congeners (EP-604 and CM-604, Tables S3–S7). As depicted in Scheme 5C, $^{1}H$ NMR spectra of products obtained from the oxidation of sulfobacin F showed two clear sets of chemical shifts each belonging to one C-6 diastereomer. While one signal set matched chemical shifts assigned to sulfonosphingolipid **27 a** and RIF-2, the second signal set exhibited chemical shift differences similar to **27 b** ($\Delta\delta_{^{1}H}$ ~0.02–0.05 ppm for 6-OH, N–H, H-3, H-4, H-5 and H-6; $\Delta\delta_{^{13}C}$ ~0.1–0.3 ppm, Tables S5 and S6). The same chemical shift patterns were obtained when NMR spectra of linear homolog **28** were compared to spectra of oxidized sulfobacin F, RIF-2, EP-604 and CM-604 (Tables S7). Based on these findings, the most likely stereochemical assignment of RIF-2 was deduced to be (2*R*,2′*R*,3*R*,6*R*) as depicted for sulfonolipid **27 a.**

### Revisiting bioactivities

Synthesized sulfonosphingolipids (**27 a**, **27 b**, **28** and the **27 a/b** mixture obtained from oxidation of sulfobacin F) were then tested for rosette-inducing activity. Despite repeated purification by high-pressure liquid chromatography (HPLC), neither **27 a**, **27 b**, **28** nor mixtures thereof induced rosette formation. Although the results were disappointing at first, the observations are in strong agreement with our activity studies of isolated RIF-like sulfonosphingolipids EP-604, CM-604, and EP-606, CM-606 as none of them induced rosette formation despite nearly identical NMR datasets.

As only RIF-1 and RIF-2 isolated from *Algoriphagus* spp. induced rosette formation, we currently hypothesize that other yet undetermined and highly potent or potentially synergizing signals might be produced by the rosette-inducing bacterium *Algoriphagus* spp.,[7] and we are currently elucidating the peculiar chemical nature of these stimulating factors. Furthermore, it can be speculated that the absolute structures of RIF-2 might still differ from synthetic **27 a** (2*R*,2′*R*,3*R*,6*R*) despite highly similar NMR pattern. Here, we acknowledge that deduction of stereochemistry in sulfonosphingolipids purely based on comparative NMR analysis requires critical evaluation as micelle formation and pH dependencies both influence $^{1}H$ and $^{13}C$ chemical shift values. Using the outlined optimized synthetic strategy current (bio)chemical studies are now directed towards the synthesis of other stereoisomers to test this hypothesis.

## Conclusion

In summary, our metabolomic and organic-synthetic driven studies resulted in three major findings. First, $HRMS^{2}$-based analysis of seven Bacteroidetes species from three different genera revealed highly similar sulfonosphingolipid profiles across species; this allowed the first isolation and structural characterization of six sulfonosphingolipid congeners from the rosette-inducing strain *C. marinum* (CM-604/606/588) and the non-inducing strain *E. pacifica* (EP-604/606/588).

Secondly, we found that the most abundant sulfonosphingolipids in *Algoriphagus*, sulfobacin D and F, inhibited RIF-related activity in a concentration-dependent manner; a similar phenomenon to that observed for the structurally related sulfonolipid IOR-1A.[7,17] This finding suggests that sulfobacins are likely competing for the same cellular target in *S. rosetta*; a finding that we will exploit for future target identification.

Thirdly, starting from a new synthetic approach of branched α-hydroxylated fatty acids, the first total syntheses of three RIF-2 isomers were accomplished in eight and 15 steps. In addition, a biomimetic synthesis of RIF-2 diastereomers through the allylic oxidation of sulfobacin F was pursued.

Detailed comparative NMR analyses of RIF-1- (RIF-1, CM-606, EP-606) and RIF-2-type sulfonosphingolipids (RIF-2, CM-604, EP-604, **27 a**/**27**, **28**) were performed and showed nearly identical chemical shift patterns; thus the same planar structure for each compound group was proposed. Based on the acquired dataset, the absolute structure of RIF-2 was tentatively assigned as 2*R*,2′*R*,3*R*,6*R*, but further biological and isolation studies are needed to solidify the assignment. The synthetic strategy and metabolic analysis established herein allow us to explore the basis of the observed structure-activity relations in this ancient predator-prey interaction in future more deeply.

## Experimental Section

The datasets supporting this article have been uploaded as part of the Supporting Information and contain details of chemical procedures, 1D and 2D NMR of described compounds, as well as HRMS data and bioassay data.

## *Acknowledgements*

We are grateful for financial support from the German Research Foundation (DFG, BE 4799/2-1). C.B. greatly acknowledges funding from the European Union's Horizon2020 research and innovation program (ERC grant no. 802736, MORPHEUS); F.U.N.R. and N.K. thank the Howard Hughes Medical Institute.

We would also like to thank Heike Heinecke (HKI) for recording the NMR spectra and Philippe Meisinger for help in the synthesis of compounds **12**. Open Access funding enabled and organized by Projekt DEAL.

## Conflict of Interest

The authors declare no conflict of interest.

## Data Availability Statement

The data that support the findings of this study are available in the supplementary material of this article.

**Keywords:** metabolomics · microbial communication · natural products · sphingolipids · total synthesis

[1] A. Woznica, N. King, *Curr. Opin. Microbiol.* **2018**, *43*, 108–116.
[2] "3.04 – Chemical Ecology of Choanoflagellates", J. P. Gerdt in *Comprehensive Natural Products III* (Eds.: H.-W. Liu, T. P. Begley), Elsevier, Oxford, **2020**, pp 45–65.
[3] M. Roper, M. J. Dayel, R. E. Pepper, M. A. R. Koehl, *Phys. Rev. Lett.* **2013**, *110*, 228104.
[4] R. A. Alegado, L. W. Brown, S. Cao, R. K. Dermenjian, R. Zuzow, S. R. Fairclough, J. Clardy, N. King, *eLife* **2012**, *1*, e00013.
[5] A. M. Cantley, J. Clardy, *Nat. Prod. Rep.* **2015**, *32*, 888–892.
[6] C. Beemelmanns, A. Woznica, R. A. Alegado, A. M. Cantley, N. King, *J. Am. Chem. Soc.* **2014**, *136*, 10210–10213.
[7] A. Woznica, A. M. Cantley, C. Beemelmanns, E. Freinkman, J. Clardy, N. King, *Proc. Natl. Acad. Sci. USA* **2016**, *113*, 7894–7899.
[8] K. Makide, H. Kitamura, Y. Sato, M. Okutani, J. Aoki, *Prostaglandins Other Lipid Mediators* **2009**, *89*, 135–139.
[9] E. V. Ireland, A. Woznica, N. King, *Appl. Environ. Microbiol.* **2020**, *86*, e02920–19.
[10] Y. A. Hannun, L. M. Obeid, *Nat. Rev. Mol. Cell Biol.* **2018**, *19*, 175–191.
[11] F. Parveen, D. Bender, S.-H. Law, V. K. Mishra, C.-C. Chen, L.-Y. Ke, *Cell Sci.* **2019**, *8*, 1573.
[12] S. T. Pruett, A. Bushnev, K. Hagedorn, M. Adiga, C. A. Haynes, M. C. Sullards, D. C. Liotta, A. H. J. Merrill, *J. Lipid Res.* **2008**, *49*, 1621–1639.
[13] J. B. Parsons, C. O. Rock, *Prog. Lipid Res.* **2013**, *52*, 249–276.
[14] E. L. Johnson, S. L. Heaver, J. L. Waters, B. I. Kim, A. Bretin, A. L. Goodman, A. T. Gewirtz, T. S. Worgall, R. E. Ley, *Nat. Commun.* **2020**, *11*, 2471.
[15] D. Leichnitz, L. Raguž, C. Beemelmanns, *Chem. Soc. Rev.* **2017**, *46*, 6330–6344.
[16] M. Wang, J. J. Carver, V. V. Phelan, L. M. Sanchez, N. Garg, Y. Peng, D. D. Nguyen, J. Watrous, C. A. Kapono, T. Luzzatto-Knaan, C. Porto, A. Bouslimani, A. V. Melnik, M. J. Meehan, W. T. Liu, M. Crüsemann, P. D. Boudreau, E. Esquenazi, M. Sandoval-Calderón, R. D. Kersten, L. A. Pace, R. A. Quinn, K. R. Duncan, C. C. Hsu, D. J. Floros, R. G. Gavilan, K. Kleigrewe, T. Northen, R. J. Dutton, D. Parrot, E. E. Carlson, B. Aigle, C. F. Michelsen, L. Jelsbak, C. Sohlenkamp, P. Pevzner, A. Edlund, J. McLean, J. Piel, B. T. Murphy, L. Gerwick, C. C. Liaw, Y. L. Yang, H. U. Humpf, M. Maansson, R. A. Keyzers, A. C. Sims, A. R. Johnson, A. M. Sidebottom, B. E. Sedio, A. Klitgaard, C. B. Larson, C. A. P. Boya, D. Torres-Mendoza, D. J. Gonzalez, D. B. Silva, L. M. Marques, D. P. Demarque, E. Pociute, E. C. O'Neill, E. Briand, E. J. N. Helfrich, E. A. Granatosky, E. Glukhov, F. Ryffel, H. Houson, H. Mohimani, J. J. Kharbush, Y. Zeng, J. A. Vorholt, K. L. Kurita, P. Charusanti, K. L. McPhail, K. F. Nielsen, L. Vuong, M. Elfeki, M. F. Traxler, N. Engene, N. Koyama, O. B. Vining, R. Baric, R. R. Silva, S. J. Mascuch, S. Tomasi, S. Jenkins, V. Macherla, T. Hoffman, V. Agarwal, P. G. Williams, J. Dai, R. Neupane, J. Gurr, A. M. C. Rodríguez, A. Lamsa, C. Zhang, K. Dorrestein, B. M. Duggan, J. Almaliti, P. M. Allard, P. Phapale, L. F. Nothias, T. Alexandrov, M. Litaudon, J. L. Wolfender, J. E. Kyle, T. O. Metz, T. Peryea, D. T. Nguyen, D. VanLeer, P. Shinn, A. Jadhav, R. Müller, K. M. Waters, W. Shi, X. Liu, L. Zhang, R. Knight, P. R. Jensen, B. Palsson, K. Pogliano, R. G. Linington, M. Gutiérrez, N. P. Lopes, W. H. Gerwick, B. S. Moore, P. C. Dorrestein, N. Bandeira, *Nat. Biotechnol.* **2016**, *34*, 828–837.
[17] A. M. Cantley, A. Woznica, C. Beemelmanns, N. King, J. Clardy, *J. Am. Chem. Soc.* **2016**, *138*, 4326–4329.
[18] D. Leichnitz, S. Pflanze, C. Beemelmanns, *Org. Biomol. Chem.* **2019**, *17*, 6964–6969.
[19] A. H. Futerman, H. Riezman, *Trends Cell Biol.* **2005**, *15*, 312–318.
[20] J. S. Yadav, V. Geetha, A. Krishnam Raju, D. Gnaneshwar, S. Chandrasekhar, *Tetrahedron Lett.* **2003**, *44*, 2983–2985.
[21] J. Chun, H.-S. Byun, R. Bittman, *J. Org. Chem.* **2003**, *68*, 348–354.
[22] A. Kováčik, J. Roh, K. Vávrová, *ChemBioChem* **2014**, *15*, 1555–1562.
[23] A. Kováčik, L. Opálka, M. Šilarová, J. Roh, K. Vávrová, *RSC Adv.* **2016**, *6*, 73343–73350.
[24] P. Wisse, M. A. R. de Geus, G. Cross, A. M. C. H. van den Nieuwendijk, E. J. van Rooden, R. J. B. H. N. van den Berg, J. M. F. G. Aerts, G. A. van der Marel, J. D. C. Codée, H. S. Overkleeft, *J. Org. Chem.* **2015**, *80*, 7258–7265.
[25] J. Spengler, F. Albericio, *Adv. Org. Synth.* **2013**, *4*, 3–35.
[26] J. T. Edwards, R. R. Merchant, K. S. McClymont, K. W. Knouse, T. Qin, L. R. Malins, B. Vokits, S. A. Shaw, D.-H. Bao, F.-L. Wei, T. Zhou, M. D. Eastgate, P. S. Baran, *Nature* **2017**, *545*, 213–218.
[27] J. Cornella, J. T. Edwards, T. Qin, S. Kawamura, J. Wang, C.-M. Pan, R. Gianatassio, M. Schmidt, M. D. Eastgate, P. S. Baran, *J. Am. Chem. Soc.* **2016**, *138*, 2174–2177.
[28] J. N. deGruyter, L. R. Malins, L. Wimmer, K. J. Clay, J. Lopez-Ogalla, T. Qin, J. Cornella, Z. Liu, G. Che, D. Bao, J. M. Stevens, J. X. Qiao, M. P. Allen, M. A. Poss, P. S. Baran, *Org. Lett.* **2017**, *19*, 6196–6199.
[29] M. Pawliczek, J. Wallbaum, D. Werz, *Synlett* **2014**, *25*, 1435–1437.
[30] M. Passiniemi, A. M. P. Koskinen, *Beilstein J. Org. Chem.* **2013**, *9*, 2641–2659.
[31] K. Matsumura, S. Hashiguchi, T. Ikariya, R. Noyori J Am, *Chem. Soc. Rev.* **1997**, *119*, 8738–8739.
[32] S. Hanashima, Y. Mizushina, T. Yamazaki, K. Ohta, S. Takahashi, H. Sahara, K. Sakaguchi, F. Sugawara, *Bioorg. Med. Chem.* **2001**, *9*, 367–376.
[33] J. Borgulya, K. Bernauer, *Synthesis* **1980**, 545–547.
[34] O. B. Wallace, D. M. Springer, *Tetrahedron Lett.* **1998**, *39*, 2693–2694.
[35] W. M. Reichert, A. Mirjafari, T. Goode, N. Williams, M. La, V. Ho, M. Yoder, J. H. Davis, *ECS Trans.* **2013**, *50*, 623–630.
[36] Only marginal $^{1}H$ and $^{13}C$ chemical-shift differences for synthetic 6*R* and 6*S*-sphingolipid building blocks were observed. To a minor degree, chemical shift differences of sulfonosphingolipids are depending on the presence of the counter ion ($NH_4^+$ vs. $nBu_4N^+$), and thus should be taken into consideration when NMR data of sulfonosphingolipids are compared (Tables S3–S7).

Manuscript received: October 27, 2021
Accepted manuscript online: December 4, 2021
Version of record online: December 28, 2021